ISSN 2176-5480

22nd International Congress of Mechanical Engineering (COBEM 2013)
November 3-7, 2013, Ribeirão Preto, SP, Brazil

EXPERIMENTAL STUDY OF NATURAL CONVECTION OF WATER IN A DIFFERENTIALLY HEATED CAVITY OF ASPECT RATIO 4

Andre R. Popinhak
Mechanical Engineering Graduate Program
Federal University of Santa Catarina
88040-900, Florianopolis, SC, Brazil
apopinhak@hotmail.com

Cesar J. Deschamps
Federal University of Santa Catarina
88040-900, Florianopolis, SC, Brazil
deschamps@polo.ufsc.br

Abstract. *This paper reports an experimental investigation of turbulent natural convection in a rectangular cavity. The cavity has an aspect ratio height/width equal to four and a square base, with the vertical walls maintained at different temperatures, resulting in a number of Rayleigh equal to 1.14 × 10^{10}. Measurements of velocity and Reynolds normal stresses were carried out via laser velocimetry Doppler (LDV) in different sections of the cavity. The flow was found to be restricted within a very narrow region next to the vertical walls, with higher levels of velocity next to the hot wall. Unexpectedly, fluid flow was seen to be upwards after a very thin layer of descending flow along the cold wall, which is probably associated with a fluid intrusion traveling upwards. The measurements also indicate the presence of vortices moving along both vertical walls.*

Keywords: *Differentially heated cavity, Natural convection, Turbulent flow*

1. INTRODUCTION

Natural convection inside a differentially heated cavity is formed by two opposing vertical walls maintained at different temperatures and the remaining walls considered to be adiabatic (Figure 1). This phenomenon is encountered in many practical applications, such as industrial cooling systems, crystal growth procedures, building insulation, and buoyancy-induced horizontal mass transfer in geophysical flows (Schöpf and Patterson, 1996).

The flow in differentially heated cavities can be fully characterized by three dimensionless parameters: the geometric aspect ratio (vertical AR_v = height/width, and horizontal AR_h = depth/width); the Prandtl number (Pr); and the Rayleigh number (Ra_H), which characterizes the flow regime as the ratio between the buoyancy and viscous forces, i.e.:

$$Ra_H = \frac{g\beta\Delta T H^3}{\nu\alpha} \tag{1}$$

In Equation (1), g is the magnitude of the gravitational field [m/s^2], β is the thermal expansion coefficient of the confined fluid [1/K], ΔT (= T_h - T_c) is the temperature difference between the two isothermal walls [K], H is the geometric characteristic length [m], taken as the cavity height, and ν and α are the kinematic viscosity [m^2/s] and the thermal diffusivity [m^2/s] of the fluid, respectively. The turbulent regime occurs at high Rayleigh numbers, and as reported by Kuyper *et al.* (1993), the laminar regime prevails for values of $Ra_H \leq 10^8$.

Thermally driven flows in differentially heated cavities is a very active area of research. However, the majority of the related literature uses bi-dimensional flow geometries. Moreover, the range of Rayleigh numbers studied is generally low, such that the fluid flow is restricted to laminar or low-level turbulence regimes (Vahl Davis and Jones, 1983; Hortmann *et al.*, 1990; Le Qéré, 1991).

Three-dimensional geometries have been studied more recently. Most works employed air-filled cavities at $Ra_H > 10^9$ (Mergui and Penot, 1997; Tian and Karayanis, 2000a; Tian and Karayanis, 2000b; Ampofo, 2004; Ampofo, 2005; Salat, 2004, Saury *et al.*, 2004). Other fluids also employed are silicone oil (Hsieh and Yang, 1996) and water (Sorias *et al.*, 2004). Such studies provided data on velocity and temperature distributions as well as turbulence quantities. Some works also obtained the heat transfer and shear stress on the isothermal walls. Schöpf and Patterson (1996) acquired a time series of images to describe flow development until the steady state is reached.

The present paper reports an experimental investigation of the turbulent natural convection of water inside an enclosed cavity with vertical aspect ratio AR_v = 4 and Rayleigh number $Ra_H \cong 10^{10}$. To the authors´ knowledge, there are no experimental measurement of velocity distribution and turbulence analysis in a water-filled cavity at this value of Rayleigh number.

ISSN 2176-5480

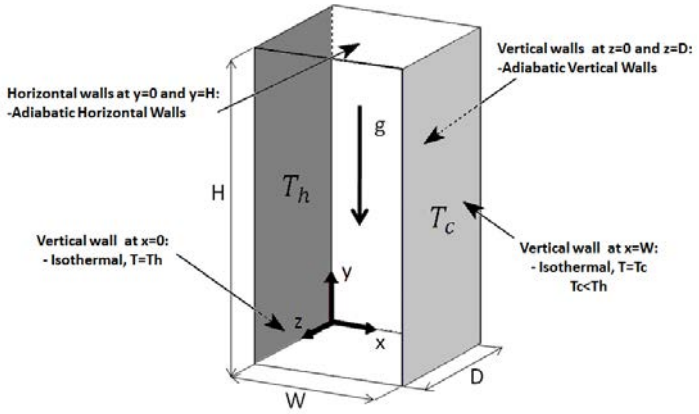

Figure 1. Schematic of a differentially heated rectangular cavity with the dimensions D × W × H (depth × width × height).

2. EXPERIMENTAL SETUP

A test rig was carefully designed and constructed in order to perform the study. Figure 2 presents a schematic diagram of the experimental apparatus, which is formed by several components: Laser Doppler Velocimetry (LDV), cavity, vibration isolator, displacement device, radiation shield, temperature control system, and temperature sensors.

2.1 Laser Doppler velocimetry (LDV)

The laser source used in the LDV system is an Argon Ion Continuous Wave (CW) Laser (Coherent Inc., model INNOVA 70C-3, 3 W power output). The separation of different color beams is made by the Fiberlight multicolor Beam Separator (TSI Inc., model FBL-3). The system output contains three pairs of beams: green (514.5 nm), blue (488 nm), and violet (476 nm). For the present work, the green and blue beams were adopted to measure the horizontal and vertical components, respectively.

The output laser from the beam separator is led to the probe TR 60 Series (TSI Inc., model TLN06-363) through the fiber optics. The signal captured is directed towards a photomultiplier that converts the optical signal into an electrical signal. This process is performed by the Photo Detector Module (PDM) (TSI, Inc., model PDM-1000). After this, the output signal from the PDM is directed to the Flow Size Analyzer (TSI, Inc., model FSA-4000) to obtain the frequencies from the electrical signals. These results are sent to a computer to evaluate flow quantities, such as velocities, turbulence quantities and so on, through use of the FlowSizer software (TSI, Inc., version 2.0.3.0).

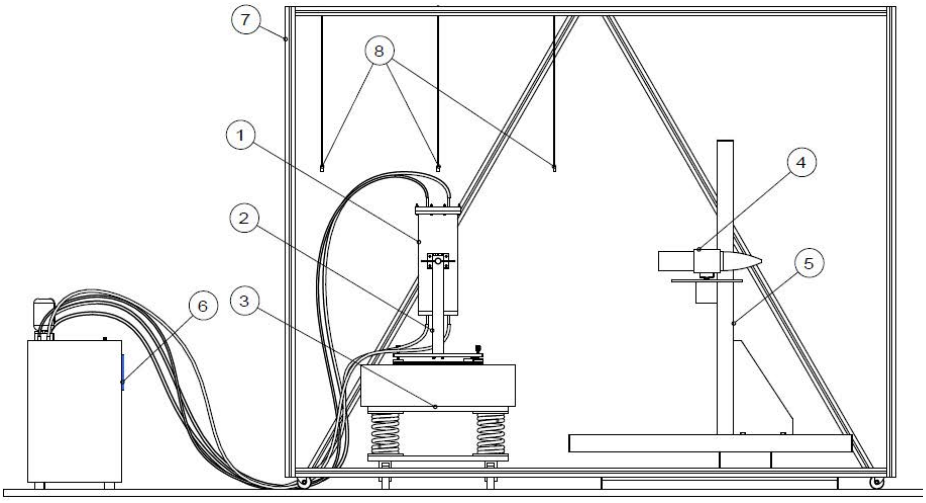

Figure 2. Experimental setup: 1) cavity; 2) support; 3) vibration isolator; 4) LDV probe; 5) displacement device; 6) thermal baths; 7) radiation shield; 8) room thermocouples

ISSN 2176-5480

2.2 Cavity

The vertical wall temperatures were fixed at 28 °C and 18 °C (T_h and T_c, respectively), and the experiment was tested in a temperature-controlled room at 23 °C. The adiabatic walls were made of acrylic because of its desired properties, such as low absorption coefficient (the laser energy losses are minimal), and low thermal conductivity. The thickness of the adiabatic walls is 32 mm. The temperature control system maintained a constant temperature to the opposite lateral walls (x = 0 and x = W) by using two thermoelectric baths (Quimis, Inc., model Q214M). The serpentine channel, combined with the high thermal capacity and thermal conductivity of the aluminum walls, allowed us to maintain them at constant and uniform temperatures.

Water was chosen as the working fluid for the experiments. It can be shown that the desired value of the Rayleigh number ($\cong 10^{10}$) is reached with H = 400 mm. The aspect ratio (height:width) of the present work is established as 4; thus, obtaining a width of 100 mm.

2.3 Temperature sensors

Temperature measurements were carried out at the cavity walls and in laboratory room by means of T-type thermocouples (Omega, Inc.). Data were recorded by a 16 channel, 24 bit, USB portable data acquisition recorder (National Instruments, Inc., model NI USB-9213), using an automatic acquisition frequency of 1.0 Hz to sample the data. The temperature readings from the thermocouples were sent via the data acquisition system to the computer by means of an interface developed in LabView 6i.

2.4 Auxiliary components

A vibration isolator system and support were designed for fixing the cavity and reducing vibration transmission from external sources by increasing the stiffness of the test rig. To reduce the natural frequency of the test rig, a 200 kg block made of concrete was attached over four isolators. A 100 kg steel plate with width, height, and depth dimensions of 650, 15, and 550 mm was attached to the top of the block. The support, which is used to hold the cavity to give stability and repeatability, has two knobs to adjust the inclination of the two horizontal axes parallel to the x and z direction.

The LDV measurement was performed by positioning the probe in different positions in order to displace the measurement volume and capture the signal from the velocity in different profiles. To displace the probe, a 3D traverse (TSI, Inc., model T3DE) was employed, which consists of a tri-axes (600 × 600 × 600 mm) displacement device controlled by a stepper motor.

2.5 Experimental procedure

The cavity was filled with water and the seeding particles were introduced before starting the heating/cooling procedure of the vertical walls. The system was left for 24 hours to reach steady state conditions, and the room illumination was turned off during the measurements to avoid noise from the light signal of the background environment.

Velocity was measured at the cavity mid-plane ($z = 0.5D$) on a very fine non-uniform mesh. First, the velocity was measured at 9 different heights and for each height, at 118 points from the hot wall to the cold wall. The first three points were 0.25, 0.38, and 0.50 mm; from 0.50 to 2 mm from the wall, the velocity was measured at every 0.25 mm; from 2 to 15.5 mm, measurement was carried out at every 0.5 mm; and from 15.5 mm to the cavity center, the distance between consecutive measuring points was 1.5 mm. Measurements were taken from the center to the cold wall, using the same coordinates but reversed. Velocity measurements were acquired at each point for a period of approximately 8 min. During all measurements, the experimental conditions were kept as steady as possible.

The laser beams entered the cavity through the acrylic wall with an inclination to the isothermal walls. Because refraction occurs as the laser beams pass through different mediums from outside to inside the cavity, such an influence was taken into account in the coordinate system. In order to take measurements near the walls, the probe had to be tilted by approximately 5 degrees. The traverse-fixed coordinate system (x, y, z) with its corresponding velocity components u, v, and w is assumed to be aligned parallel to the wall. In the present work, a four-beam two-velocity system was employed, and a transformation was used for the horizontal velocity component u.

Experimental repeatability was verified by measuring a half profile on the hot wall side to the center of the cavity at $Y = 0.5$ and $Z = 0.5$. The three dimensionality of the flow was analyzed by comparing the velocity distribution at two different cavity depths, Z = 0.5 and 0.95. The expanded uncertainty for measurements of temperature is 0.2 ^{o}C. For a confidence level of 95%, the expanded uncertainty of the Rayleigh number is $U_{Ra} = 2.96 \times 10^8$, which represents 2.6% of the specified value for the experiment ($Ra_H \cong 10^{10}$). The uncertainty associated with measurements of velocity is typically less than 0.5% of the measured value.

ISSN 2176-5480

3. RESULTS AND DISCUSSION

3.1 Velocity field

Measurements of the mean vertical velocity component at different heights and Z = 0.5 are shown in Figure 3, respectively. In order to avoid the overlap of the data, constants were added in the vertical axis. The parameter V_o is the buoyancy velocity, defined as $V_o = [g\beta W (T_h - T_c)]^{1/2}$, and is used as a normalization parameter for the velocity and turbulence intensity results. In the present flow situation, V_o = 0.04851 m/s, and W is the distance between the heated and cold walls. As can be seen, a boundary layer starts at the bottom of the hot wall and its thickness increases as it reaches the upper region of the cavity. In contrast, the boundary layer along the cold wall starts at the top with a thinner thickness, which increases as it reaches the bottom region. The flow can be divided into two distinct regions: (i) the wall region where the velocity gradients are high; (ii) the core region where the flow is approximately stationary. As can be seen, higher velocities are obtained near the hot wall region, and the peak velocities of the hot side are around three times greater than the velocities of the cold side.

Figure 4 shows results for vertical and horizontal velocity components next to the cold and heated walls at three different vertical positions: Y = 0.2, 0.5 and 0.8. The maximum vertical velocity reaches its value of 8.43 mm/s at cavity mid-height (Y = 0.5, where $Y = y/H$) at X = 0.025. Analyzing the vertical velocity profiles of the hot wall side shows that outside the boundary layers there are small negative velocities at Y = 0.5 and 0.8, suggesting a clockwise recirculating motion. An unexpected result is obtained in the region of the cold wall. Initially, there is a thin film of water of the order of 1–1.5 mm descending on the cold wall. The flow has a tendency to turn its direction upwards after this thin film, and within this region the flow reaches a positive vertical velocity in the top-cold region at Y = 0.5–0.8. Beyond the boundary layer on the cold wall, the fluid is moving upwards, reaching positive velocities throughout most of the cavity height. Following a nomenclature adopted by Hsieh and Yang (1996), this phenomenon is referenced as an intrusion traveling upwards. The horizontal components of velocity are approximately anti-symmetrical at Y = 0.5. It can be noticed a significant dispersion in the measurements for horizontal velocity component at Y = 0.2. A zoomed view of the vector velocity shown for the cold side region in Figure 5 suggests an intrusion upwards in the flow field.

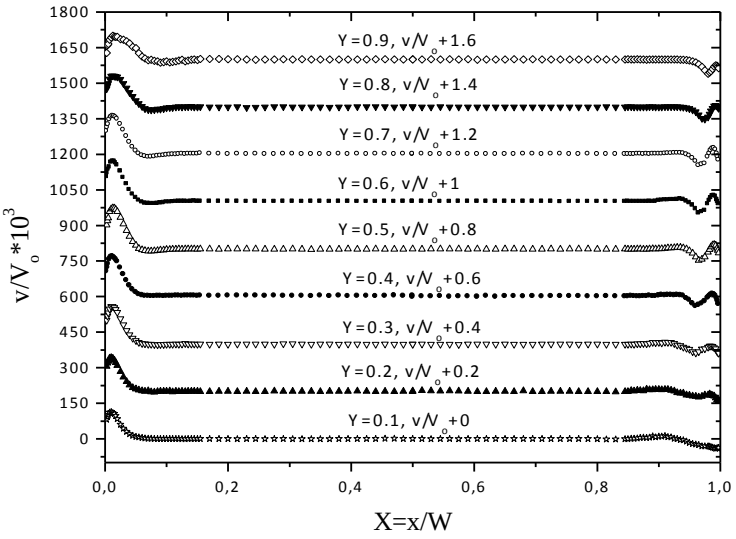

Figure 3. Profiles of average vertical velocity component at different heights.

Three-dimensional effects associated with variation of properties across the cavity may be the responsible for the flow asymmetry seen in Figures 3 and 4. The smaller viscosity in the vicinity of the hot wall also leads to a larger upward velocity than the velocity near the cold wall. The asymmetry was also observed by Hsieh and Yang (1996) using silicon oil as the working fluid (Pr = 457), and $Ra_H = 6.9 \times 10^7 - 4.12 \times 10^8$ in a rectangular cavity.

The anti-symmetrical flow feature was observed in the studies of natural convection in air-filled cavities carried out by Soria *et al*. (2004) through DNS, in a cavity with aspect ratio 4 and $Ra_H = 6.4 \times 10^8$, and experimentally by Tian and Karayiannis (2000a, 2000b) with a square cavity $Ra_H = 1.58 \times 10^9$. According to Gifford (1991), the anti-symmetrical feature disappears in non-Boussinesq solutions. Gray and Giorgini (1976) pointed out that the use of the Boussinesq approximation in the momentum equations could be considered valid for variations of thermophysical properties up to 10% with respect to the mean value. The working conditions of this work presented a variation of about 12% in the dynamic viscosity and 22% of the thermal expansion coefficient.

ISSN 2176-5480

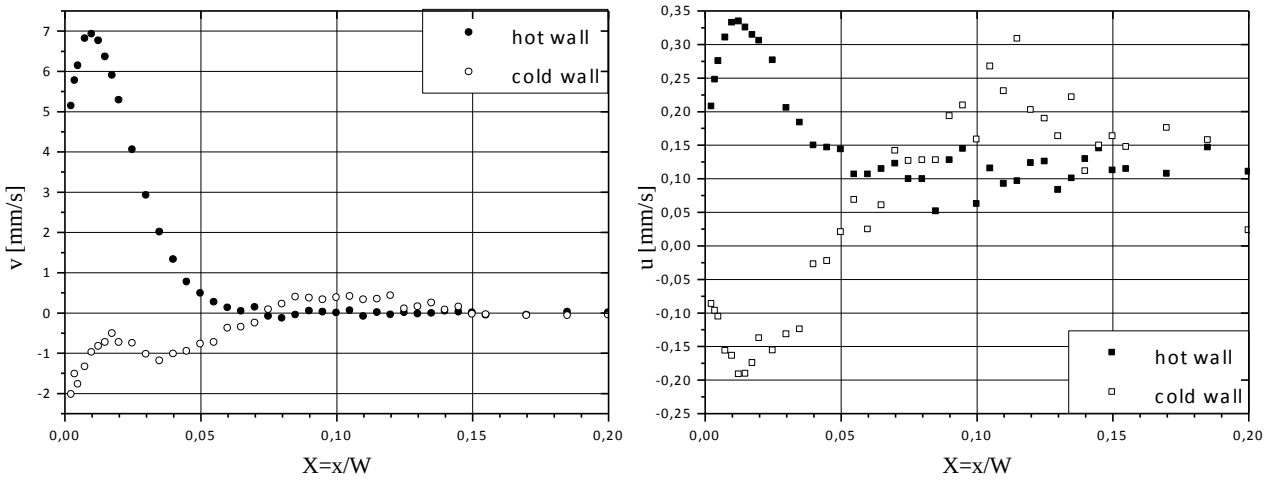

(a)

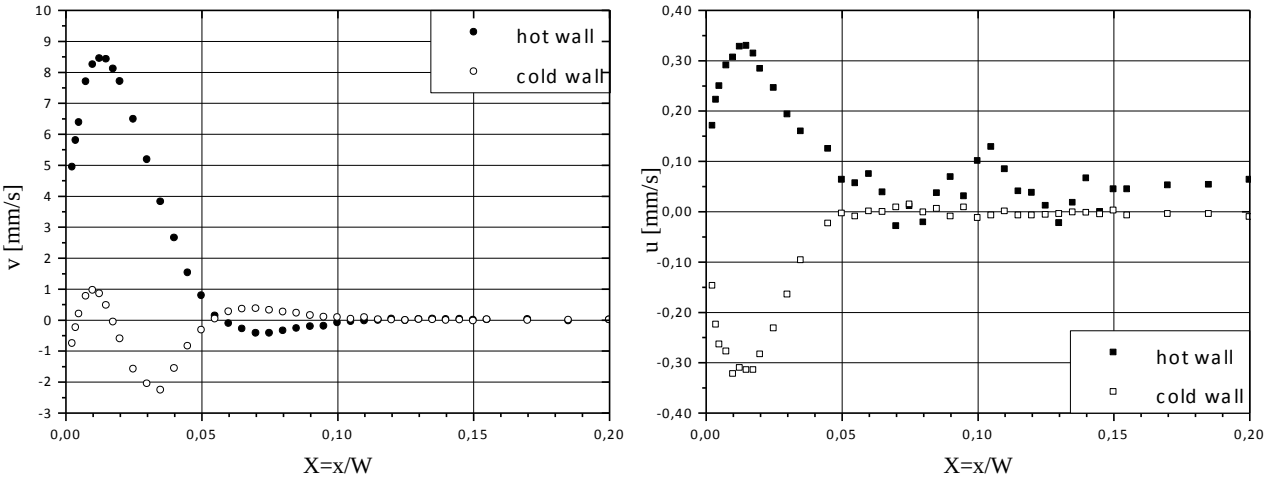

(b)

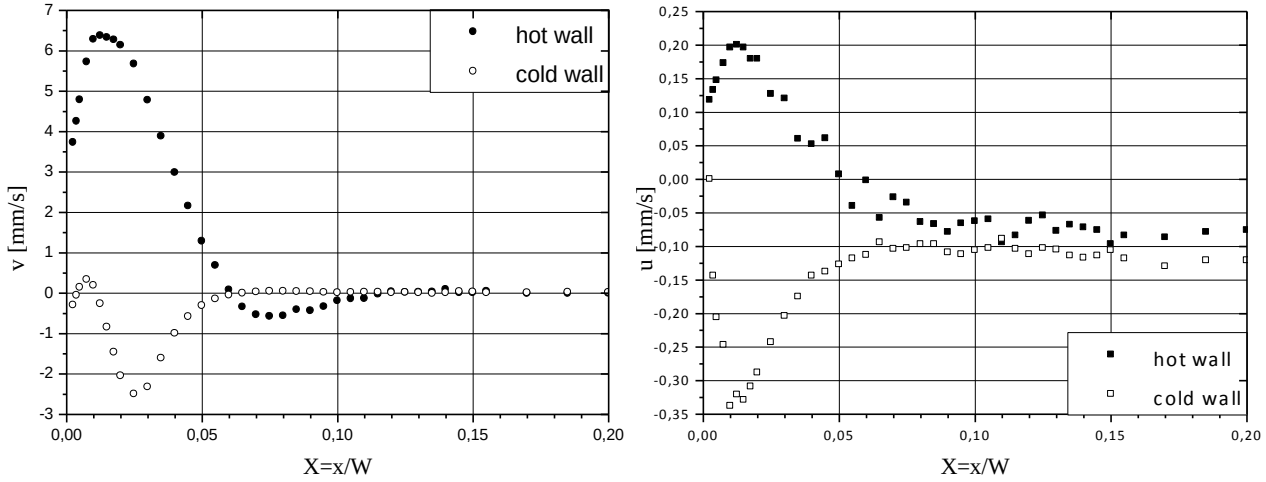

(c)

Figure 4. Vertical and horizontal components of average velocity: (a) Y = 0.2; (b) Y = 0.5; (c) Y = 0.8.

ISSN 2176-5480

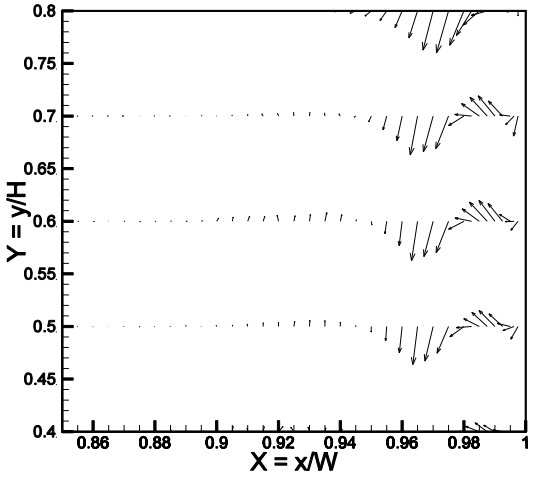

Figure 5. Velocity vectors at the mid-height region on the cold wall side.

3.2 Turbulence field

The vertical and horizontal components of the root-mean-square (rms) velocity fluctuations at different heights are shown in Figure 6. As expected, the fluctuations are higher in the top-left and bottom-right regions. Overshoots in the rms profiles can be noticed at Y = 0.3, 0.6 and Y = 0.9.

The rms velocity fluctuations near the hot and cold walls are shown in Figure 7. On the hot wall side, turbulence anisotropy is verified from the wall up to X ≅ 0.05, with the maximum condition occurring at X ≅ 0.018 ($v'_{rms}/u'_{rms} \approx$ 2.5). On the cold wall side, the maximum anisotropy is reached at $X \cong 0.98$ ($v'_{rms}/u'_{rms} \approx 4$). The turbulence anisotropy decreases towards the core region of the cavity where the fluid is virtually motionless.

The turbulent kinetic energy, k, can be estimated as

$$k = \frac{1.5\left(u'^2 + v'^2\right)}{2} \tag{2}$$

Figure 8 shows contours of turbulent intensity I ($= \sqrt{2k/3}/V_o$), considering the buoyancy velocity (V_o) as the normalization parameter. The peak turbulence intensity occurs near the hot wall, although a larger region affected by turbulence is present along the cold wall. The chosen range of colors adopted in Figure 8 does not allow one to clearly identify the region of highest turbulent intensity (I = 1.5–2.4%) within a small region close to Y = 0.9 and between X = 0.015–0.065.

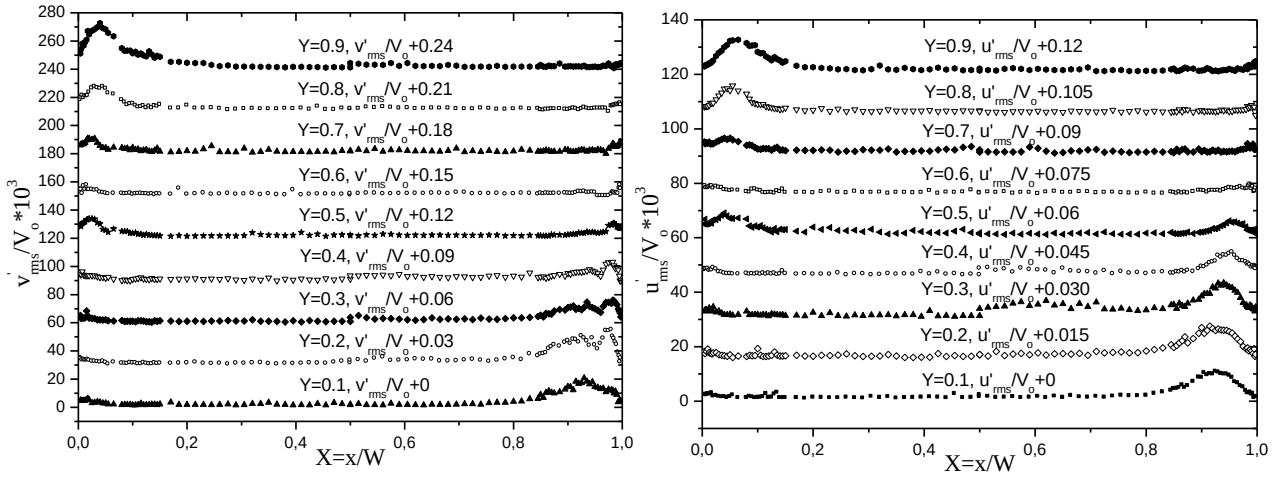

(a) (b)

Figure 6. Vertical and horizontal components of the rms velocity fluctuations at different heights.

ISSN 2176-5480

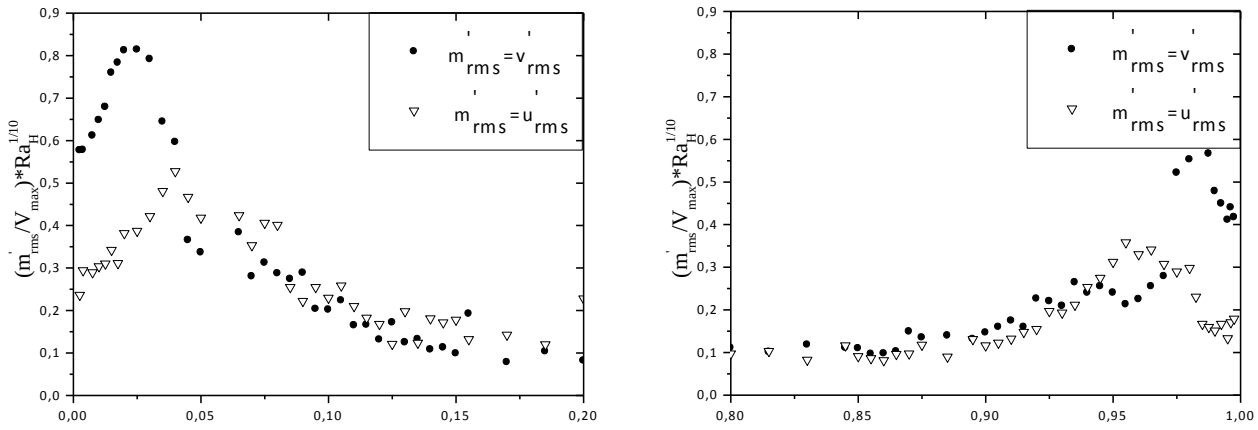

(a) (b)

Figure 7. Reynolds normal stresses near the walls at Y = 0.5: (a) hot wall side; (b) cold wall side.

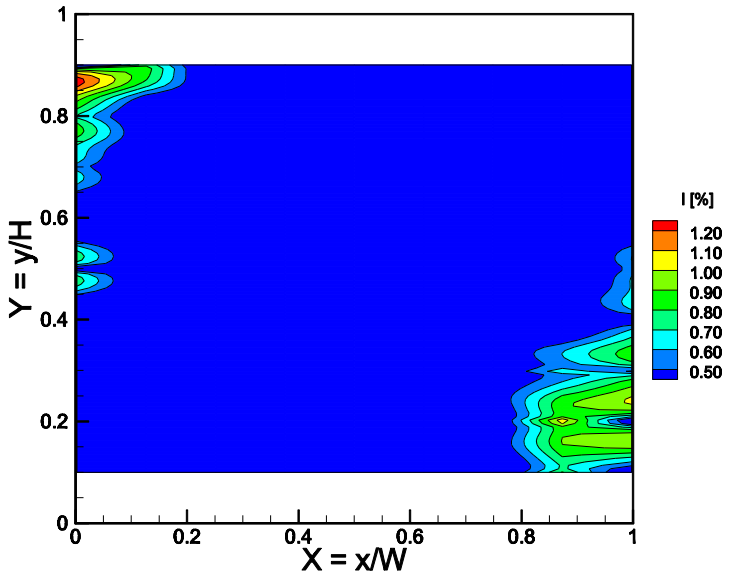

Figure 8. Contours of turbulent kinetic energy.

4. CONCLUSIONS

The experimental data for velocity showed that the flow is limited to a small portion in the near-wall region, which represents only 10% of the domain within the heated walls direction. The core region of the cavity is approximately stationary. If compared with an air-filled cavity, the boundary layer is thinner in the same conditions. The peak velocities occur approximately in the region Y = 0.5–0.6. The turbulence was found to be more intense where the vertical boundary layer is thicker, i.e., in top hot and bottom cold regions. The flow presented an asymmetrical feature, where higher velocities were observed on the hot wall side. An unexpected result was obtained in the cold wall region where, immediately after a very thin film of descending water, the flow occurs upwards very near the wall.

5. ACKNOWLEDGEMENTS

The material presented herein has been partially funded by CNPq (Brazilian Research Council) through Grant No. 573581/2008-8 (National Institute of Science and Technology in Refrigeration and Thermophysics) and CAPES (Coordination for the Improvement of High Level Personnel.

6. REFERENCES

Schöpf, W. and Patterson, J.C., 1996, “Visualization of natural convection in a side-hetaed cavity: transition to the final steady state”, *Int. J. Heat Mass Transfer*, Vol. 39, p. 3497-3509.

ISSN 2176-5480

Kuyper, R.B. , Van der Meer, T.H.H. , Hoogendoorn, C.J. and Henkes, R.B.W.M., 1993, "Numerical study of laminar and turbulent natural convection in an inclined square cavity", *Int. J. Heat Mass Transfer*, Vol. 36, pp. 2899 – 2911.

Vahl Davis, G. and Jones, I.P., 1983, "Natural convection in a square cavity: a comparison exercise", *Int. J. Numer. Meth. Fluids*, Vol. 3, pp. 227-248.

Hortmann, M., Peric, M. and Scheuerer, G., 1990, "Finite volume multigrid prediction of laminar natural convection: bench-mark solutions", *Int. J. Numer. Meth. Fluids*, Vol. 11, pp. 189-207.

Le Quéré, P., 1991, "Accurate solutions to the square thermally driven cavity at high Rayleigh number", *Comput. Fluids*, Vol. 20, pp. 29–41.

Mergui, S. and Penot, F., 1997, "AnalysIe des vitesse et température de l´air en convection naturelle dans une cavité carrée différentiellement chauffée à Ra = 1.69 x 10^9", *Int. J. Heat Mass Transfer*, Vol. 40, pp. 3427-3441.

Tian, Y.S. and Karayiannis, T.G., 2000a, "Low turbulence natural convection in an air cavity filled square cavity - Part I: the thermal and fluid flow fields", *Int. J. Heat Mass Transfer*, Vol. 43, pp. 849-866.

Tian, Y.S. and Karayiannis, T.G., 2000b, "Low turbulence natural convection in an air filled square cavity - Part II: the turbulence quantities", *Int. J. Heat Mass Transfer*, Vol. 43, pp. 867-884.

Ampofo, F., 2004, "Turbulent natural convection in an air filled partitioned square cavity", *Int. J. Heat Fluid Flow*, Vol. 25, pp. 103-114.

Ampofo, F., 2005, "Turbulent natural convection of air in a non-partitioned or partitioned cavity with differentially heated vertical and conducting horizontal walls", *Exp. Therm. Fluid Sci.*, Vol. 29, pp. 137-157.

Salat, J., 2004, "Experimental and numerical investigation of turbulent natural convection in a large air-filled cavity", *Int. J. Heat Fluid Flow*, Vol. 25, pp. 824-832.

Saury, D., Rouger, N., Djanna, F. and Penot, F., 2011, "Natural convection in an air-filled cavity: Experimental results at large Rayleigh numbers", *Int. Commun. Heat Mass Transfer*, Vol. 38, pp. 679-687.

Hsieh, S.S. and Yang, S.S., 1996, "Transient three-dimensional natural convection in a rectangular enclosure", *Int. J. Heat Mass Transfer*, Vol. 39, pp. 13-26.

Soria, M., Trias, F.X., Perez-Segarra, C.D. and Oliva, A., 2004, "Direct Numerical Simulation of a Three-Dimensional Natural-Convection Flow in a Differentially Heated Cavity of Aspect Ratio 4", *Numer. Heat Transfer, Part A*, Vol. 45, pp. 649-673.

Gifford, A.W., 1991, "Natural Convection in a square cavity without the Boussinesq Approximation", In: *Proceedings of the 49th Annual Technical Conference - ANTEC´91*, Montréal, pp. 2448-2454.

Gray, D.D. and Giorgini, A., 1976, "The validity of the boussinesq approximation for liquids and gases", *Int. J. Heat Mass Transfer*, Vol. 19, pp. 545-551

7. RESPONSIBILITY NOTICE

The authors are the only responsible for the printed material included in this paper.